SYNTHETIC BIOLOGY

Synthetic Signal Propagation Through Direct Cell-Cell Interaction

Mitsuhiro Matsuda,[1,2] Makito Koga,[1,2] Eisuke Nishida,[2] Miki Ebisuya[1]*

Contact-dependent cell communication has the potential to generate elaborate cell patterns, and this occurs in vivo. We used the Delta-Notch signaling system, consisting of the ligand Delta and the receptor Notch, to construct a positive feedback loop between adjacent cells to generate a propagating signal in cultured cells. To amplify the responses of Notch to Delta, we created a cell-cell positive feedback loop using an engineered transcriptional cascade and a Notch positive regulator, Lunatic fringe. We used mathematical modeling to determine the appropriate amount of amplification to enable the induction of Delta to propagate from one cell to its neighboring cells, which generated bistability within the local cell populations and resulted in discrete groups of cells that were either positive or negative for Delta. These results demonstrate the sufficiency of the cell-cell positive feedback loop to generate signal propagation and cell population–level bistability. This study represents a step in engineering more elaborate cell patterns in mammalian cells.

INTRODUCTION

Cell-cell communication is essential to coordinate cellular behavior within populations. Various types of synthetic cell-cell communication have been reported, including interspecies communication (*1*), synchronized oscillation among cells (*2*), cell population density control through cell-cell communication (*3*), and the formation of ring or stripe patterns (*4*, *5*). These synthetic cell-cell communication systems used secreted molecules as the signal transducer. Multicellular organisms use both secreted molecules and signaling through direct cell-cell contact to communicate.

A typical example of such a contact-dependent form of communication is Notch signaling, where both Delta (the ligand) and Notch (the receptor) are transmembrane proteins, and the ligand-receptor binding between adjacent cells causes the release of the Notch intracellular domain (NICD) within the cells (*6*, *7*) (Fig. 1A). The NICD translocates to the nucleus where it acts as a transcriptional regulator. This NICD-mediated transcriptional regulation between adjacent cells contributes to controlling cell differentiation and to generating patterns of cells in tissues (*8*–*11*). Because contact-dependent transcriptional regulation works at the resolution of single cells, the Notch signaling system can be used to create systems with finer control of cell populations compared with the diffusion-dependent systems. The Notch signaling system can also involve positive feedback among adjacent cells (*12*–*16*). For example, in the inner ear of developing vertebrates, binding of Jagged1 (Jag1, another Notch ligand) to Notch between adjacent cells promotes production of Jag1 itself (*14*–*16*). This Jag1-Notch positive feedback loop among adjacent cells has been suggested to contribute to propagating Jag1 production to the neighboring cells and maintaining the regions consisting of cells with a uniformly high amount of Jag1 (*14*–*16*). However, no studies have tested whether the cell-cell positive

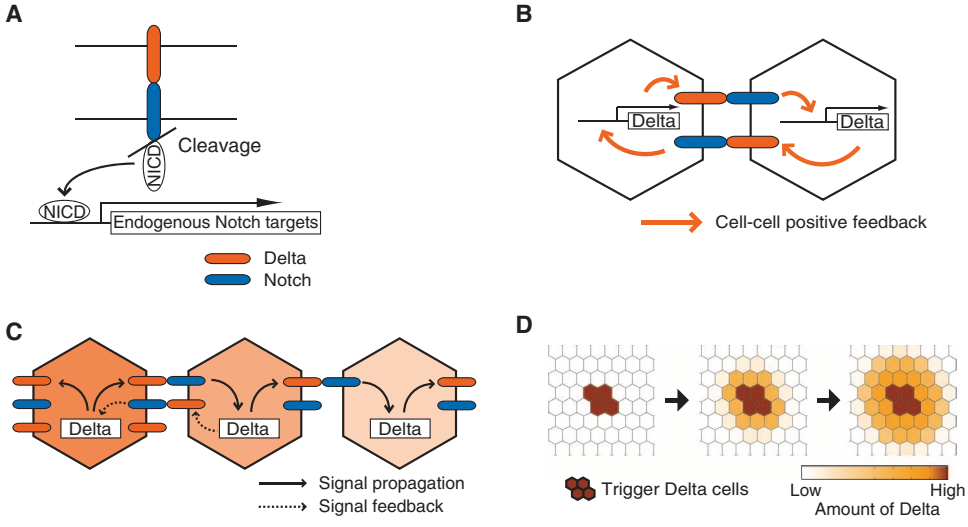

Fig. 1. Scheme for synthetic signal propagation. (**A**) Schematic diagram of the endogenous Delta-Notch signaling pathway. Delta induces proteolytic cleavage of Notch and release of the Notch intracellular domain (NICD), which enters the cell nucleus to mediate gene expression. (**B**) Scheme for a cell-cell positive feedback loop. In our genetic circuits, one cell that expresses Delta promotes the expression of Delta in the other cell through Delta-Notch signaling. The mutual activation mechanism between the adjacent cells forms a cell-cell positive feedback loop upon direct cell-cell interaction. (**C**) Scheme for signal propagation. A cell producing a high level of Delta (the first cell) induces the expression of Delta in the adjacent cell. Then, the adjacent cell (the second cell) induces Delta expression in the third cell. In addition, the second cell also induces Delta expression in the first cell (signal feedback). (**D**) 2D view of the signal propagation. The Trigger cells that constantly produce a high amount of Delta induce the expression of Delta in the adjacent cells. The sequential induction of Delta expression results in a signal propagation pattern.

[1]Career-Path Promotion Unit for Young Life Scientists, Kyoto University, Sakyo-ku, Kyoto 606-8501, Japan. [2]Department of Cell and Developmental Biology, Graduate School of Biostudies, Kyoto University, Sakyo-ku, Kyoto 606-8502, Japan. *To whom correspondence should be addressed. E-mail: ebisuya@lif.kyoto-u.ac.jp

feedback loop of Notch signaling is sufficient to generate such a coordinated behavior of the cell population.

Therefore, we used the Notch signaling system and synthesized a circuit (Fig. 1B) that produced a propagating signal in cultured mammalian cells (Fig. 1, C and D). In our constructed genetic circuits, all cells were positive for Notch and also responded to binding of Delta to Notch with transcription of a Delta-encoding plasmid (Fig. 1B). Thus, a cell that produced Delta forced the adjacent cells to produce Delta. This mutual activation between adjacent cells (the cell-cell positive feedback loop) produced bistability at the level of local cell populations when the feedback loop satisfied certain conditions: The system generated either a region consisting of cells with a uniformly high amount of Delta or a region with a uniformly low amount of Delta, depending on the initial conditions. Furthermore, by placing "Trigger Delta cells," which constantly produced a high amount of Delta, in the region of cells with a low amount of Delta, the cell-cell positive feedback system produced a transition from the low to the high Delta state: the production of Delta propagated from the Trigger cells to the neighboring cells (Fig. 1, C and D).

This kind of synthetic biology approach is useful to test the mechanistic sufficiency of genetic circuits. Here, we found that the cell-cell positive feedback loop of Notch signaling is sufficient to generate a propagating signal. We also found that the genetic circuit requires appropriate amplification to achieve signal propagation. The ability to engineer contact-dependent signals that propagate is an important step toward finer control of cell populations and generation of more elaborate cell patterns in mammalian cells and tissues.

RESULTS

Circuit design and amplification of the Notch response

To design the circuit, we wanted to create a simple system and minimize variables that could affect the outcome through unknown mechanisms. Because many genes can be affected by Notch signaling and thus introduce unnecessary and potentially confounding complexity in our system, we replaced the NICD with an orthogonal transcription factor (a bacterial transcription activator), tTA (tetracycline-controlled transactivator) (*17*, *18*), and introduced this construct by lentiviral infection into Madin-Darby canine kidney (MDCK) cells and Chinese hamster ovary (CHO) cells (Fig. 2A). These cell types do not express endogenous *Delta*, and the expression of endogenous *Notch* is less than that of the exogenous chimeric protein, Notch-tTA (fig. S1). We also monitored the response to Notch activation with a reporter construct containing the gene encoding luciferase (Luc) under the control of a tTA-responsive element (TRE-Luc). When the Notch-tTA–producing cells were cocultured with the Trigger cells, a reporter construct containing the luciferase gene under the control of a TRE-Luc exhibited a fourfold increase in the luciferase activity relative to that of Notch-tTA–producing cells cocultured with MDCK cells that were not Delta-positive (wild-type cells). Thus, the chimeric protein Notch-tTA was functional (Fig. 2B, 1-step).

We created simple mathematical models that are based on ordinary differential equations with Hill functions to simulate the behavior of the genetic circuits. Our simulation results were consistent with previous reports (*19*–*21*) and showed that a multistep cascade amplified the response to the input signal over a wide range of the parameter values (Fig. 2C, compare the 1-step with the 2-step). Therefore, we modified the structure of the genetic circuit by constructing a two-step circuit to amplify the response of Notch to the Trigger cells. In the two-step circuit, the released tTA activated another transcription activator, Gal4VP16 (GV), and the resulting GV activated a luciferase reporter containing a Gal4 upstream activator sequence (UAS-Luc) (Fig. 2A and fig. S2). In agreement with the simulation results, the luciferase reporter of the two-step circuit exhibited a larger activity (16-fold) when the cells were cocultured with the Trigger cells (Fig. 2B, two-step). The luciferase activities in the two-step and one-step circuits were almost the same (1.2-fold versus 1-fold) when the cells were cocultured with wild-type cells. To further amplify the response of Notch,

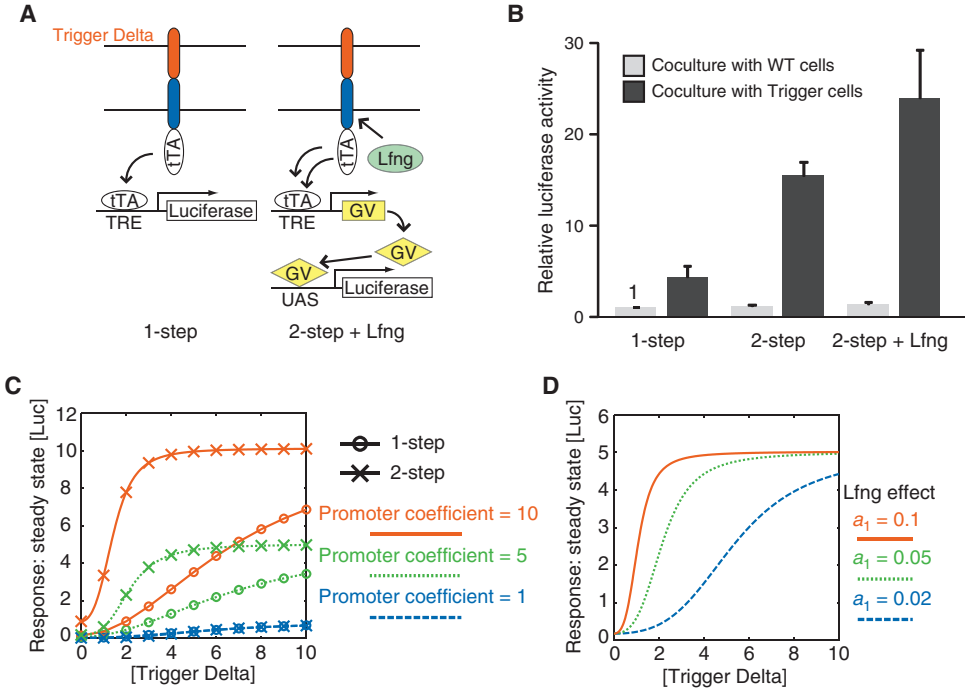

Fig. 2. Circuit design and amplification of the Notch response. (**A**) The NICD was replaced with tTA. In a one-step circuit, the released tTA induces the expression of luciferase (1-step). In a two-step circuit, the tTA induces the expression of Gal4VP16 (GV), and GV induces the expression of luciferase (2-step). Lfng was introduced to enhance Notch activation (2-step + Lfng). (**B**) The cells engineered with each circuit were cocultured with either Trigger or wild-type (WT) cells and assayed for luciferase activity. The activity values were normalized to the value of one-step circuit cells cocultured with the WT cells. Data are means + SEM. $n = 6$. (**C**) Simulated steady-state responses to Trigger Delta of one-step or two-step circuits. The three lines with the circles are the responses of three hypothetical one-step circuits with different promoter coefficients. The three lines with the cross marks are the responses of two-step circuits with different promoter coefficients. The TRE and UAS promoter coefficients correspond to the parameters c1 and c2 in the model, respectively. (**D**) Simulated steady-state responses to Trigger Delta of two-step circuits with different sensitivities of Notch activation. Lfng is assumed to increase the sensitivity, which corresponds to the parameter a_1 in the model.

we introduced a glycosyltransferase, Lunatic fringe (Lfng), into the two-step circuit (Fig. 2A and fig. S2). Lfng modifies Notch and enhances its sensitivity to Delta-induced activation (*22*, *23*). In agreement with the simulation results (Fig. 2D), the luciferase reporter exhibited a larger activity (24-fold) when used with Lfng and still maintained a relatively low basal response (1.4-fold) (Fig. 2B, two-step + Lfng).

Identification of the combinations of the two promoters and Lfng that create population-level bistability and signal propagation

Using the mathematical models, we investigated the conditions that should lead to signal propagation. We focused on the "coefficient" of the promoters as a tunable parameter. Because we introduced the genetic circuits into the cells with lentiviral vectors, the copy numbers of the promoters differ among the clonal cell lines. The insertion of the lentiviral constructs into different loci also leads to differences in long-range transregulatory influences on the promoters. Furthermore, the inserted lentiviral constructs often suffer from silencing by methylation. We introduced the term "promoter coefficient" to represent the differences in the promoters caused by these aggregate effects. Our simulation results showed that propagating signals were achievable with the two-step circuit, but not with the one-step circuit, when the same promoter coefficients were assumed for both circuits (Fig. 3, A to D). The simulation results also showed that a proper combination of the coefficients of the two promoters in the two-step circuit (the TRE promoter and the UAS promoter) was critical for signal propagation (Fig. 3, C and D). The two-step circuits that had at least one small promoter coefficient failed to generate a region with a high abundance of Delta in response to the Trigger cells (Fig. 3, C and E, the bottom left "Inactive" regions). The two-step circuits that had a combination of two large promoter coefficients generated a region with a uniformly high amount of Delta even in the absence of the Trigger cells (Fig. 3, D and E, the top right "Hyperactive" regions). The two-step circuits that had a combination of two intermediate promoter coefficients generated signal propagation patterns (Fig. 3, C and E, the "Propagation" region).

The conditions for signal propagation closely resembled those for the population-level bistability (fig. S3). Unlike our previous simulations (Fig. 3), which assessed the signal propagation from the Trigger cells to the neighboring cells, the Trigger-less model does not contain the Trigger cells and was used to calculate a bifurcation diagram. The bifurcation diagram showed that the two-step circuits have two stable steady states (bistable) or one steady state (monostable), depending on the combination of the promoter coefficients (fig. S3). We found that the bistable region in the bifurcation diagram was almost the same as (slightly larger than) the Propagation region calculated in the previous simulations (fig. S3). This can be explained intuitively as follows. For signal propagation, the cells must initially exist in the state with a low amount of Delta in the absence of the Trigger cells and then, in the presence of the Trigger cells, the cells must move into the state with higher amounts of Delta and maintain the high state. Therefore, the genetic circuits for signal propagation must have two stable steady states. We also found that the

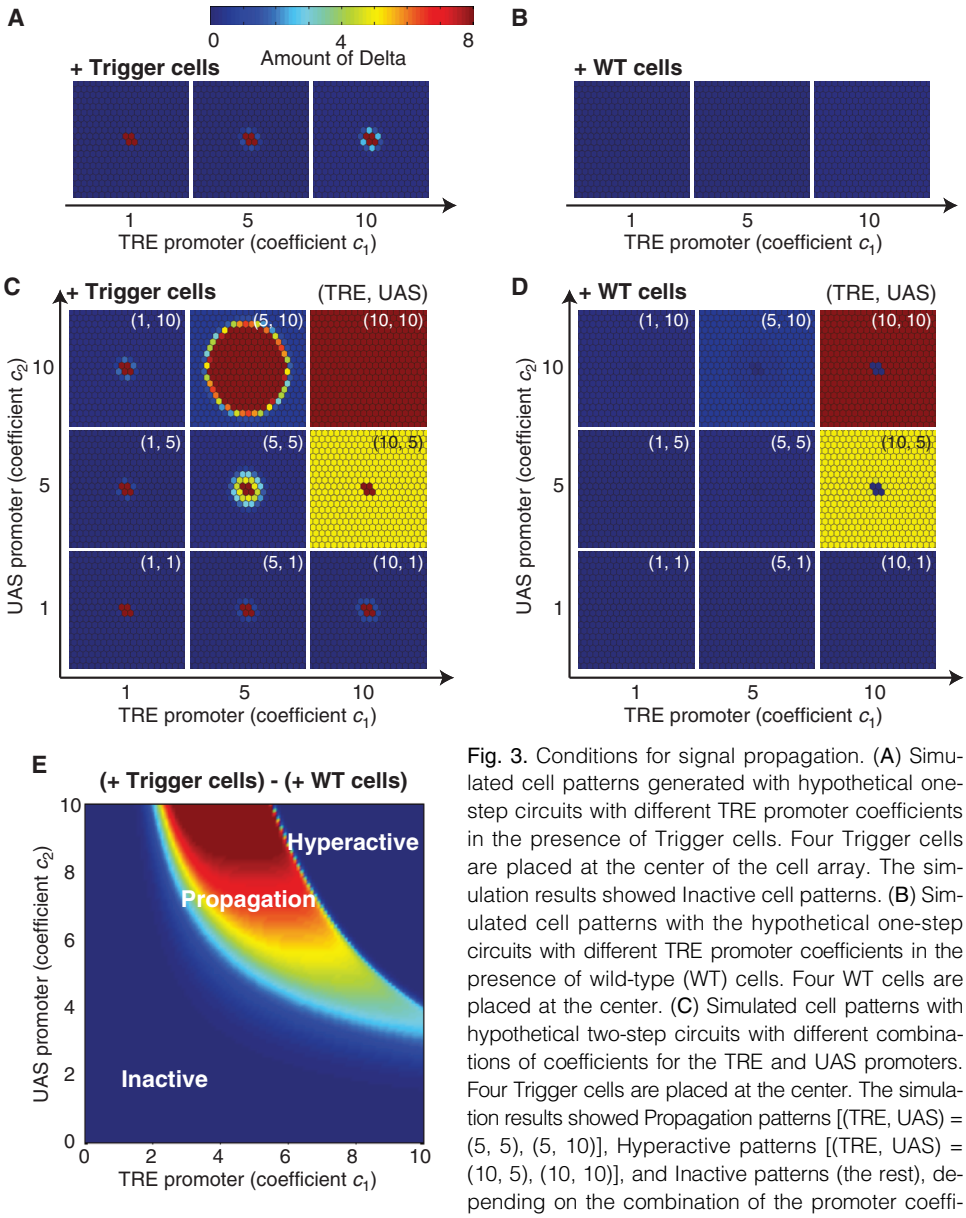

Fig. 3. Conditions for signal propagation. (**A**) Simulated cell patterns generated with hypothetical one-step circuits with different TRE promoter coefficients in the presence of Trigger cells. Four Trigger cells are placed at the center of the cell array. The simulation results showed Inactive cell patterns. (**B**) Simulated cell patterns with the hypothetical one-step circuits with different TRE promoter coefficients in the presence of wild-type (WT) cells. Four WT cells are placed at the center. (**C**) Simulated cell patterns with hypothetical two-step circuits with different combinations of coefficients for the TRE and UAS promoters. Four Trigger cells are placed at the center. The simulation results showed Propagation patterns [(TRE, UAS) = (5, 5), (5, 10)], Hyperactive patterns [(TRE, UAS) = (10, 5), (10, 10)], and Inactive patterns (the rest), depending on the combination of the promoter coefficients. (**D**) Simulated cell patterns with the hypothetical two-step circuits with different combinations of coefficients for the TRE and UAS promoters in the presence of WT cells. Four WT cells are placed at the center. (**E**) Heat map representing the amount of Delta in the simulated cell patterns with the Trigger cells minus that with the WT cells. The amount of Delta in a cell in the third row from the Trigger cells at 30 hours was used. The warm colors indicate the region of signal propagation in the parameter space.

introduction of Lfng shifted the bistable region so that the bistability and signal propagation were achievable with smaller promoter coefficients (fig. S3).

Characterization of clonal cell lines engineered with each genetic circuit

To experimentally confirm the predictions from the simulations, we constructed a cell-cell positive feedback loop based on the initial one- and two-step circuits, but we replaced the luciferase reporter with Delta. To visualize the production of Delta, we linked Delta to a green fluorescent protein (GFP) reporter (Delta-2A–GFP, a construct for bicistronic expression of Delta and GFP using the viral 2A peptide) (*24*, *25*). The ability of Delta-2A–GFP construct to function as a Notch ligand was comparable to that of the original Delta construct (fig. S4).

The CHO cells engineered with the one-step (Notch-tTA and TRE–Delta-2A–GFP) or two-step (Notch-tTA, TRE-GV, and UAS–Delta-2A–GFP) circuits were cocultured with either Trigger cells or wild-type cells and analyzed by flow cytometry. The response of the GFP reporter exhibited variability among the cell clones, probably as a result of the different combination of the promoter coefficients. To obtain an appropriate combination of the promoter coefficients, we isolated several cell clones for the one- and two-step circuits. Most of the one-step circuit cell clones (32 of 35 clones) did not respond to the Trigger cells (Fig. 4A, one-step, Weak response). In a few one-step circuit clones (3 of 35 clones), about 10% of

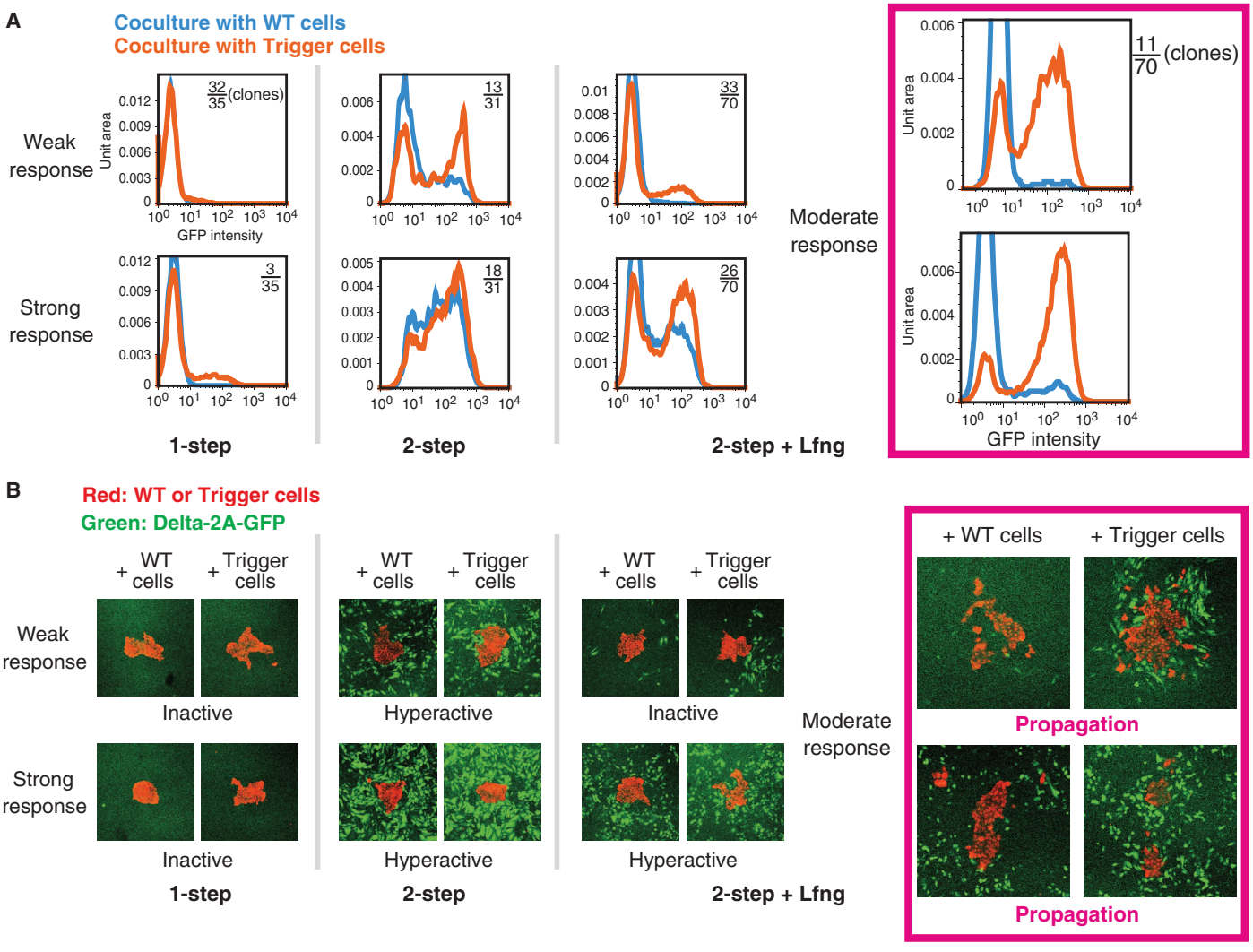

Fig. 4. Responses and cell patterns in clonal cell lines. (**A**) Clonal lines of CHO cells engineered with either one-step, two-step, or two-step + Lfng, were cocultured with either Trigger or WT CHO cells at a ratio of 1:9. The GFP intensities were measured by fluorescence-activated cell sorting (FACS). Thirty-five cell clones engineered with one-step circuit were classified into "Weak response" and "Strong response" (left). Thirty-one cell clones with two-step circuit were classified into "Weak response" and "Strong response" (middle). Seventy cell clones with two-step + Lfng circuit were classified into "Weak response," "Strong response," and "Moderate response" (right). The representative clones are shown. The numbers of clones in these categories are shown. Two clones representing the Moderate response group are outlined in pink. (**B**) The clonal CHO cells shown in (A) were cocultured with either Trigger or WT MDCK cells at a ratio of 1000:1. The Trigger and WT cells were labeled with monomeric Kusabira Orange 2 (mKO2) and plated 2 days before. A signal propagation pattern was observed in the two Moderate response clones (outlined in pink).

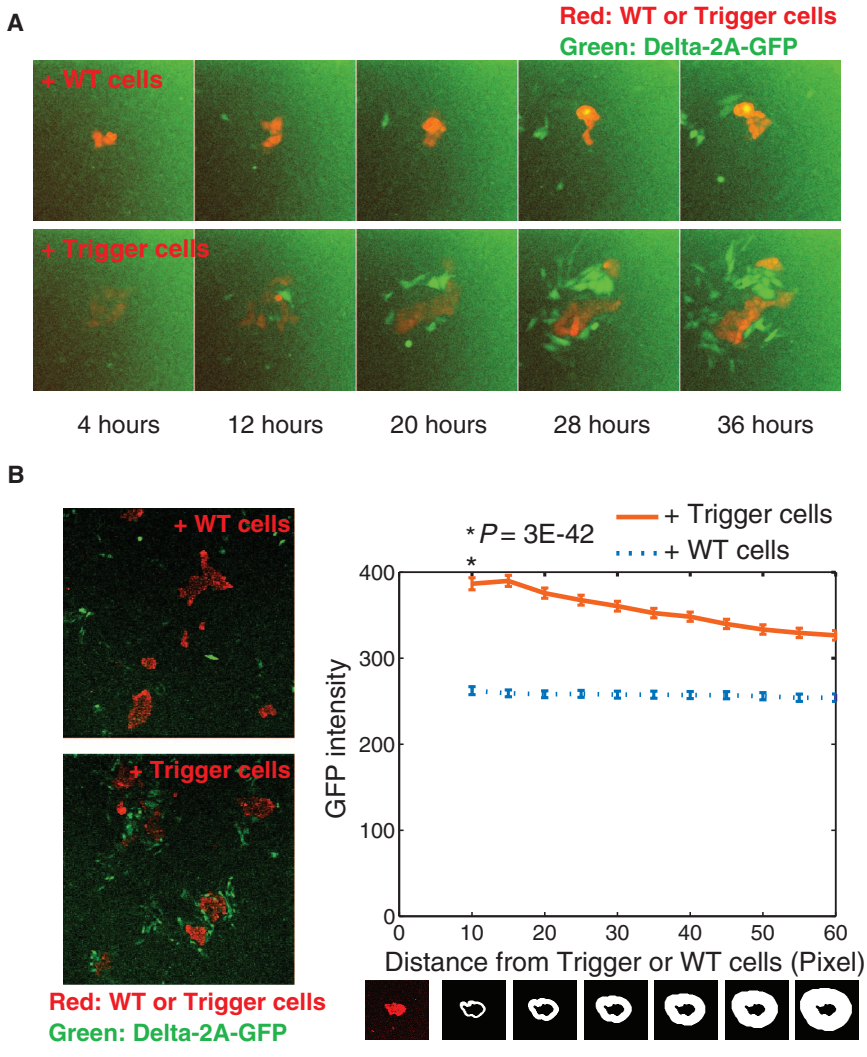

Fig. 5. Synthesis of a signal propagation pattern. (**A**) Time-lapse imaging of signal propagation. The clonal CHO cells engineered with two-step + Lfng (a Moderate response line) were cocultured with either Trigger or WT MDCK cells at a ratio of 1000:1. The Trigger and WT cells were labeled with mKO2. The GFP signal gradually propagated from the Trigger cells to the neighboring cells (see movie S1). (**B**) Quantification of the signal propagation. Wide-range images of the propagation pattern were taken 40 hours after coculture (left, partial images are shown). Average GFP intensities were calculated for the regions around the Trigger or WT MDCK cells (right). The boxes below the graph represent an example of each quantified region. The average GFP intensity decreased according to the distance from the Trigger cells. Data are means ± SEM. n = 100 to 300 regions around the Trigger or WT cells. The P value (calculated by Student's t test) for only in the closest point to the Trigger cells (at 10 pixels) is provided. (**C**) Time-lapse imaging of signal propagation with the cells aligned in a row. The clonal CHO cells engineered with two-step + Lfng (a Moderate response line) were cocultured with the Trigger MDCK cells at a ratio of 20:1 on a micropatterned cultureware. The GFP signal propagated along the row. The arrow indicates the GFP-positive cells that spontaneously emerged in distant regions from the Trigger cells. This time-lapse imaging corresponds to the Region_1 in movie S2.

the cell population became GFP-positive when the cells were cocultured with the Trigger cells (Fig. 4A, one-step, Strong response), indicating that the production of Delta was induced. However, the induction of Delta was not strong enough to cause propagation, and most of the cells remained GFP-negative even around the Trigger cells (an Inactive cell pattern) (Fig. 4B, one-step). All the Strong response clones engineered with the one-step circuit resulted in the Inactive cell pattern.

In agreement with the results with the luciferase reporters and the simulations, the GFP intensities in the two-step circuit cell clones were stronger than those in the one-step circuit clones, indicating that the two-step cascade amplified the response to the Trigger cells (Fig. 4A, compare the one-step with the two-step). Although one-third of two-step circuit clones (10 of 31 clones) still did not respond to the Trigger cells, a few clones (3 of 31 clones) showed a bimodal distribution of GFP intensity in response to the Trigger cells (Fig. 4A, two-step, Weak response). On the other hand, none of the one-step circuit clones showed such bimodal distribution. In most of the two-step circuit clones (18 of 31 clones), however, the GFP reporter showed strong intensity, and more than 50% of the cell population became GFP-positive even when the clones were cocultured with the wild-type cells instead of Trigger cells (Fig. 4A,

two-step, Strong response). As a result, there were GFP-positive cells all over the place irrespective of the Trigger cells (a Hyperactive cell pattern) (Fig. 4B, two-step). Even the two-step circuit clones that showed bimodal distribution resulted in the Hyperactive cell pattern (Fig. 4B, two-step, Weak response).

In the cell clones engineered with the two-step circuit and Lfng, one-third (21 of 70 clones) did not respond to the Trigger cells. In one-fifth of two-step + Lfng clones (12 of 70 clones), less than 40% of the cell population became GFP-positive in response to the Trigger cells (Fig. 4A, two-step + Lfng, Weak response). The Weak response clones with two-step + Lfng showed the Inactive cell pattern (Fig. 4B, two-step + Lfng, Weak response). In one-third of the clones (26 of 70 clones), more than 30% of the cell population became GFP-positive even in the absence of the Trigger cells (Fig. 4A, two-step + Lfng, Strong response). The Strong response clones showed the Hyperactive cell pattern (Fig. 4B, two-step + Lfng, Strong response). The two-step + Lfng clones exhibited bimodal distributions more frequently (25 of 70 clones) than did the two-step clones (3 of 31 clones). The simulation results suggested that Lfng makes the input-response curves steeper (Fig. 2C), which could generate switch-like behavior and the lack of cells exhibiting an intermediate response, and this induces the high frequency of the bimodal distribution. Furthermore, the response to the wild-type cells was kept low in the two-step + Lfng clones (Fig. 4A, compare the blue lines of two-step with that of two-step + Lfng). We classified these bimodal and low background clones as "Moderate response" clones (11 of 70 clones) (Fig. 4A, two-step + Lfng, Moderate response). In the Moderate response clones, about 70 to 80% of the cell population became GFP-positive in response to the Trigger cells, and less than 30% became GFP-positive in response to the wild-type cells (Fig. 4A, two-step + Lfng, Moderate response). Two Moderate response clones showed a propagated signal, generating demarcated GFP-positive regions around the Trigger cells (Fig. 4B, two-step + Lfng, Moderate response).

Signal propagation

We visualized the signal propagation process in the Moderate response cell clones engineered with the genetic circuit of two-step + Lfng (Fig. 5A, + Trigger cells and movie S1). GFP-positive cells initially emerged among the cells directly in contact with the Trigger cells. Later, the GFP signal increased in a region a few cell diameters away from the Trigger cells, indicating that the signal to produce Delta signal had propagated to the neighboring cells. In contrast, the GFP signal remained low around the wild-type cells (Fig. 5A, + WT cells and movie S1). As a result, GFP-positive cell regions (the cells near the Trigger cells) and GFP-negative cell regions (the cells distant from the Trigger cells) were generated (Fig. 5B, + Trigger cells), suggesting that the cell population had two stable steady states (bistable). To further facilitate visualization of the signal propagation process, we aligned the cells in a row with micropatterned cultureware (Fig. 5C and movie S2). The GFP signal propagated along the row from the Trigger cells to the neighboring cells. As a result, the GFP-positive cells formed in a line, showing that the signal propagated along the aligned cells. Occasionally, GFP-positive cells emerged even in distant regions from the Trigger cells probably as a result of the natural fluctuations in gene expression (Fig. 5C). This resulted in the propagation of the GFP signal from the spontaneously active region to the neighboring cells.

DISCUSSION

Here, we synthesized a cell-cell positive feedback loop based on contact-dependent cell signaling in mammalian cells. The genetic circuit structure (the two-step circuit) and Lfng contributed to amplifying the response and to generating the switch-like behavior of the cell-cell positive feedback system. Whereas a cell-autonomous positive feedback loop is known to generate the bistability within the cell (*26*–*29*), our cell-cell positive feedback loop generated the bistability of local cell populations. When the conditions for the population-level bistability were satisfied, the signal propagated from the Trigger cells to the neighboring cells. These results suggested that the cell-cell positive feedback loop of Notch signaling, such as the Jag1-Notch positive feedback loop in vivo (*14*–*16*), is sufficient for propagating a signal and keeping the signal high in mammalian cells.

It should be noted, however, that our signal propagation in cultured cells was not uniform compared to the simulated signal propagation pattern. Even in the cells adjacent to the Trigger cells, there was always a fraction of nonresponding cells. This is probably due to inhomogeneous gene silencing by methylation or natural fluctuations in gene expression. Lentiviral constructs are also susceptible to trans-regulatory effects of endogenous enhancers. Targeted integration of genetic materials into specific integration sites or usage of chromatin insulator will help mitigate these undesirable (and uncontrollable) effects on gene expression. In our time-lapse imaging, cell movement and division further perturbed the signal propagation pattern. In addition, the propagation stopped after reaching a few cell diameters for unknown reasons. Therefore, to achieve a finer signal propagation cell pattern, we need to find a way of controlling these factors.

The contact-dependent cell communication described in this study has the potential to generate more elaborate and complex cell patterns, such as a salt-and-pepper pattern and a boundary between cells (*7*, *9*). Reconstituting these cell patterns in mammalian cultured cells will provide unique opportunities to test the mechanistic sufficiency of current models of pattern formation and to discover out missing elements in the models. Furthermore, it should be possible to regulate cell differentiation in specified regions by replacing the GFP reporter with master regulators of cell differentiation in the future. Again, there are many technical challenges. Implementing genetic circuits in a suitable cell type is important. For example, the CHO cells used in this study are known for genome instability and chromosome rearrangements, which are not suitable for long-term culture. Certain biological phenomena, such as cell differentiation, occur only in specific types of cells, such as stem cells, which can be difficult to handle. Another confounding concern is that the synthetic genetic circuits could perturb endogenous signaling pathways in unintended ways and vice versa. Caution and efforts to prevent undesirable crosstalk and off-target effects are necessary, such as the replacement of the NICD with a bacterial transcription factor. Therefore, this study is at the beginning of overcoming these difficulties and synthesizing genetic circuits at will.

MATERIALS AND METHODS

DNA constructs

Notch (residues 1 to 1752 of mouse Notch1), Delta (mouse Dll1), Lfng (mouse Lfng), tTA (tTA-Advanced, Clontech), luciferase (pGL4.10, Promega), CANotch-GV (gift from G. Struhl), GV, TRE (pTRE-Tight, Clontech), and UAS (pSwitch, Invitrogen) complementary DNAs (cDNAs) were subcloned into pDONR to construct entry vectors according to the manufacturer's protocol (Invitrogen). The stop codon was removed from the sequence of Delta, Lfng, GV, and CANotch-GV to fuse the ORF (open reading frame) in-frame with a C-terminal V5 tag. These entry clones were recombined with pLenti6.3 (Invitrogen) by means of the Multisite Gateway technology (Invitrogen). To produce the Delta-2A–GFP construct, we linked the sequences of Delta (containing V5 tag) and enhanced GFP to the 2A peptide sequence encoded by 5′-CGCGCCAAGCGCGGCTCCGGCCAGTGCACCAACTACGCCCTGCTGAAGCTGGCCGGCGACGTGGAGTCCAACCCCGGCCCC-3′.

Culture protocols

MDCK cells were maintained in Dulbecco's modified Eagle's medium (DMEM) containing 10% fetal bovine serum (FBS). CHO cells were maintained in DMEM/F12 medium containing 10% FBS.

Generation of stable cell lines

Viruses for each individual pLenti construct were generated according to the manufacturer's protocols (Invitrogen). MDCK or CHO cells were transduced for 24 hours. At the end of transduction, the supernatants were removed and cells were maintained in basal medium plus blasticidin (10 μg/ml), puromycin (1 μg/ml), hygromycin (200 μg/ml), or zeocin (200 μg/ml) for the selection of drug-resistant clones.

Reporter assay

The MDCK cells stably infected with each genetic circuit were cocultured with either Trigger or wild-type MDCK cells at a density of 4×10^5 cells per well in a 12-well plate. After 36 hours of coculture, luciferase activities were measured according to the manufacturer's protocols (Promega).

Western blotting

Western blotting was performed by means of standard protocols. The blot was probed with mouse anti-V5 antibody (Invitrogen).

Quantitative reverse transcription–polymerase chain reaction

Whole-cell RNA was extracted with an RNA easy kit (Qiagen), and reverse-transcribed with the QuantiTect Reverse Transcription Kit (Qiagen). Polymerase chain reaction (PCR) was then performed with the LightCycler 480 II (Roche). The measured value was normalized to glyceraldehyde-3-phosphate dehydrogenase (GAPDH). Primers were designed in the mRNA sequences where the parts of the sequences are identical between mouse and dog, or mouse and hamster. The primers for the PCR analysis are as follows: Delta (MDCK), 5′-TTCCCCTTCGGCTTCACCTG-3′ and 5′-CGGCTGATGAGTCTTTCTGG-3′; Delta (CHO), 5′-CTGGGTG-TCGACTCCTTCAG-3′ and 5′-GGGCTTCAATGATCAGAGAG-3′; Notch (MDCK), 5′-GCAAAGCCATCTGCACCT-3′ and 5′-CTCATC-CACGTCCTGGCT-3′; Notch (CHO), 5′-GCAAAGCCATCTGCACCT-3′ and 5′-CTCATCCACGTCCTGGCT-3′; GAPDH (MDCK), 5′-CAT-CAACGGGAAGTCCATCT-3′ and 5′-TACTCAGCACCAGCATCACC-3′; and GAPDH (CHO), 5′-TGGGTGTGAACCAAGACAAG-3′ and 5′-CCTTCCACAATGCCAAAGTT-3′.

Models

We constructed simple mathematical models that represented the processes of tTA release upon Delta-Notch binding, production of GV, and production of Delta (or luciferase). The models are based on ordinary differential equations with Hill functions. The following equations were used to simulate the steady-state responses of the two-step circuits:

$$\frac{dT}{dt} = a_1 D_T - d_1 T$$

$$\frac{dG}{dt} = c_1\left(b_1 + \frac{a_2 T^{n_1}}{K_1^{n_1} + T^{n_1}}\right) - d_2 G$$

$$\frac{dD}{dt} = c_2\left(b_2 + \frac{a_3 G^{n_2}}{K_2^{n_2} + G^{n_2}}\right) - d_3 D$$

The variables are D_T (Trigger Delta), T (tTA), G (GV), D (output Delta or luciferase) (μM). The following parameters were used: $a_2 = a_3 = 0.7$ (μM/hour); $b_1 = b_2 = 0.01$ (μM/hour); $d_1 = d_2 = d_3 = 0.7$ (/hour); $K_1 = K_2 = 0.5$ (μM); $n_1 = n_2 = 2$. The variations in promoter coefficients (due to the different copy numbers and different loci) are represented by the parameters c_1 and c_2 (the default value used is 5). Lfng is assumed to enhance the sensitivity of Notch activation and therefore increase the parameter a_1 (the default value used is 0.05/hour).

In the case of the one-step circuits, the following equations were used:

$$\frac{dT}{dt} = a_1 D_T - d_1 T$$

$$\frac{dD}{dt} = c_1\left(b_1 + \frac{a_2 T^{n_1}}{K_1^{n_1} + T^{n_1}}\right) - d_2 D$$

To simulate signal propagation in a two-dimensional (2D) array of hexagonal cells, we used D_m (the average expression level of Delta in the six adjacent cells) instead of D_T:

$$D_m(j,k) = \frac{1}{6}\{D(j,k+1) + D(j+1,k+1) + D(j-1,k) + D(j+1,k) + D(j-1,k-1) + D(j,k-1)\}$$

where j and k are the indices of the cell array. Four Trigger or wild-type cells that produce a constant amount of Delta (7 or 0 μM/hour) were placed at the center of the cell array. The equations were solved on 32×32 cell arrays with periodic conditions by means of Matlab's ode45 solver (MathWorks). The bifurcation diagrams were produced by XPPAUT.

Fluorescence-activated cell sorting analysis

After the clonal CHO cells engineered with each genetic circuit were maintained in the medium containing doxycycline (Dox; 1 ng/ml) for 1 to 3 days, the CHO cells were cocultured with either Trigger or wild-type CHO cells at a density of 3×10^5 cells per well in a 12-well plate. After 24 hours of coculture in the absence of Dox, the cells were trypsinized and analyzed for GFP fluorescence with the FACSCalibur (Becton Dickinson) and FlowJo software.

Image and data analysis

After the clonal CHO cells engineered with two-step + Lfng were maintained in the medium containing Dox (1 ng/ml) for 1 to 3 days, the CHO cells were cocultured with either Trigger or wild-type MDCK cells in the absence of Dox. The Trigger and wild-type cells were plated 2 days before the addition of the engineered cells. To align the cells in a row, we plated the CHO cells and the Trigger MDCK cells on micropatterned cultureware, CytoGraph (DNP). Movies were acquired with an incubator microscope system (LCV110, Olympus) and images were acquired with a confocal microscope system (FV1000, Olympus). Data collection and analysis were performed with MetaMorph software (Molecular Devices).

SUPPLEMENTARY MATERIALS

www.sciencesignaling.org/cgi/content/full/5/220/ra31/DC1
Fig. S1. Quantification of endogenous Delta and Notch transcripts.
Fig. S2. Characterization of the genetic circuits.
Fig. S3. Bistability and signal propagation.
Fig. S4. The ability of Delta-2A–GFP to function as a ligand for Notch.
Movie S1. Time-lapse imaging of signal propagation.
Movie S2. Time-lapse imaging of signal propagation using the cells aligned in a row.

REFERENCES AND NOTES

1. W. Weber, M. Daoud-El Baba, M. Fussenegger, Synthetic ecosystems based on airborne inter- and intrakingdom communication. *Proc. Natl. Acad. Sci. U.S.A.* **104**, 10435–10440 (2007).

2. T. Danino, O. Mondragón-Palomino, L. Tsimring, J. Hasty, A synchronized quorum of genetic clocks. *Nature* **463**, 326–330 (2010).
3. L. You, R. S. Cox III, R. Weiss, F. H. Arnold, Programmed population control by cell-cell communication and regulated killing. *Nature* **428**, 868–871 (2004).
4. S. Basu, Y. Gerchman, C. H. Collins, F. H. Arnold, R. Weiss, A synthetic multicellular system for programmed pattern formation. *Nature* **434**, 1130–1134 (2005).
5. C. Liu, X. Fu, L. Liu, X. Ren, C. K. Chau, S. Li, L. Xiang, H. Zeng, G. Chen, L. H. Tang, P. Lenz, X. Cui, W. Huang, T. Hwa, J. D. Huang, Sequential establishment of stripe patterns in an expanding cell population. *Science* **334**, 238–241 (2011).
6. E. H. Schroeter, J. A. Kisslinger, R. Kopan, Notch-1 signalling requires ligand-induced proteolytic release of intracellular domain. *Nature* **393**, 382–386 (1998).
7. S. J. Bray, Notch signalling: A simple pathway becomes complex. *Nat. Rev. Mol. Cell Biol.* **7**, 678–689 (2006).
8. S. Artavanis-Tsakonas, M. D. Rand, R. J. Lake, Notch signaling: Cell fate control and signal integration in development. *Science* **284**, 770–776 (1999).
9. J. Lewis, Notch signalling and the control of cell fate choices in vertebrates. *Semin. Cell Dev. Biol.* **9**, 583–589 (1998).
10. P. Heitzler, P. Simpson, The choice of cell fate in the epidermis of *Drosophila*. *Cell* **64**, 1083–1092 (1991).
11. J. R. Collier, N. A. Monk, P. K. Maini, J. H. Lewis, Pattern formation by lateral inhibition with feedback: A mathematical model of Delta-Notch intercellular signalling. *J. Theor. Biol.* **183**, 429–446 (1996).
12. J. F. de Celis, S. Bray, Feed-back mechanisms affecting Notch activation at the dorsoventral boundary in the *Drosophila* wing. *Development* **124**, 3241–3251 (1997).
13. V. M. Panin, V. Papayannopoulos, R. Wilson, K. D. Irvine, Fringe modulates Notch–ligand interactions. *Nature* **387**, 908–912 (1997).
14. B. H. Hartman, T. A. Reh, O. Bermingham-McDonogh, Notch signaling specifies prosensory domains via lateral induction in the developing mammalian inner ear. *Proc. Natl. Acad. Sci. U.S.A.* **107**, 15792–15797 (2010).
15. N. Daudet, J. Lewis, Two contrasting roles for Notch activity in chick inner ear development: Specification of prosensory patches and lateral inhibition of hair-cell differentiation. *Development* **132**, 541–551 (2005).
16. W. Pan, Y. Jin, B. Stanger, A. E. Kiernan, Notch signaling is required for the generation of hair cells and supporting cells in the mammalian inner ear. *Proc. Natl. Acad. Sci. U.S.A.* **107**, 15798–15803 (2010).
17. D. Sprinzak, A. Lakhanpal, L. Lebon, L. A. Santat, M. E. Fontes, G. A. Anderson, J. Garcia-Ojalvo, M. B. Elowitz, Cis-interactions between Notch and Delta generate mutually exclusive signalling states. *Nature* **465**, 86–90 (2010).
18. G. Struhl, A. Adachi, Nuclear access and action of Notch in vivo. *Cell* **93**, 649–660 (1998).
19. D. Karig, R. Weiss, Signal-amplifying genetic circuit enables in vivo observation of weak promoter activation in the Rhl quorum sensing system. *Biotechnol. Bioeng.* **89**, 709–718 (2005).
20. S. Hooshangi, S. Thiberge, R. Weiss, Ultrasensitivity and noise propagation in a synthetic transcriptional cascade. *Proc. Natl. Acad. Sci. U.S.A.* **102**, 3581–3586 (2005).
21. M. Thattai, A. van Oudenaarden, Attenuation of noise in ultrasensitive signaling cascades. *Biophys. J.* **82**, 2943–2950 (2002).
22. C. Hicks, S. H. Johnston, G. diSibio, A. Collazo, T. F. Vogt, G. Weinmaster, Fringe differentially modulates Jagged1 and Delta1 signalling through Notch1 and Notch2. *Nat. Cell Biol.* **2**, 515–520 (2000).
23. T. M. Kato, A. Kawaguchi, Y. Kosodo, H. Niwa, F. Matsuzaki, Lunatic fringe potentiates Notch signaling in the developing brain. *Mol. Cell. Neurosci.* **45**, 12–25 (2010).
24. M. L. Donnelly, G. Luke, A. Mehrotra, X. Li, L. E. Hughes, D. Gani, M. D. Ryan, Analysis of the aphthovirus 2A/2B polyprotein 'cleavage' mechanism indicates not a proteolytic reaction, but a novel translational effect: A putative ribosomal 'skip.' *J. Gen. Virol.* **82**, 1013–1025 (2001).
25. M. D. Ryan, J. Drew, Foot-and-mouth disease virus 2A oligopeptide mediated cleavage of an artificial polyprotein. *EMBO J.* **13**, 928–933 (1994).
26. J. J. Tyson, K. C. Chen, B. Novak, Sniffers, buzzers, toggles and blinkers: Dynamics of regulatory and signaling pathways in the cell. *Curr. Opin. Cell Biol.* **15**, 221–231 (2003).
27. A. Becskei, B. Séraphin, L. Serrano, Positive feedback in eukaryotic gene networks: Cell differentiation by graded to binary response conversion. *EMBO J.* **20**, 2528–2535 (2001).
28. W. Xiong, J. E. Ferrell Jr., A positive-feedback-based bistable 'memory module' that governs a cell fate decision. *Nature* **426**, 460–465 (2003).
29. F. J. Isaacs, J. Hasty, C. R. Cantor, J. J. Collins, Prediction and measurement of an autoregulatory genetic module. *Proc. Natl. Acad. Sci. U.S.A.* **100**, 7714–7719 (2003).

Acknowledgments: We thank G. Struhl for the CANotch-GV construct. **Funding:** This work was supported by grants from the Funding Program for Next Generation World-Leading Researchers (NEXT Program), Grant-in-Aid for Young Scientists (Start-up), and the Special Coordination Fund for Promoting Science and Technology. **Author contributions:** M.M. and M.E. designed the study and wrote the manuscript with the help of E.N.; M.M. performed most of the experiments; M.K. conducted a part of luciferase assays and quantitative reverse transcription–PCR analyses; M.E. conducted modeling and simulations; and M.E. and E.N. supervised the project. **Competing interests:** The authors declare that they have no competing financial interests.

Submitted 12 December 2011
Accepted 29 March 2012
Final Publication 17 April 2012
10.1126/scisignal.2002764
Citation: M. Matsuda, M. Koga, E. Nishida, M. Ebisuya, Synthetic signal propagation through direct cell-cell interaction. *Sci. Signal.* **5**, ra31 (2012).

Synthetic Signal Propagation Through Direct Cell-Cell Interaction

Mitsuhiro Matsuda, Makito Koga, Eisuke Nishida and Miki Ebisuya

(April 10, 2012)
Science Signaling **5** (220), ra31. [doi: 10.1126/scisignal.2002764]
originally published online April 10, 2012

Science Signaling (ISSN 1937-9145) is published weekly, except the last December, by the American Association for the Advancement of Science, 1200 New York Avenue, NW, Washington, DC 20005.